BUREAU INTERNATIONAL
DES POIDS ET MESURES

On-site comparison of Quantum Hall Effect resistance standards of the NMC A*STAR and the BIPM

Ongoing key comparison BIPM.EM-K12

Report on the March 2019 on-site comparison

Final report, September 2021

P. Gournay*, B. Rolland*,
S.W. Chua**, K.H. Lim** and E. Tan**

* Bureau International des Poids et Mesures (BIPM)
** National Metrology Centre, A*STAR (Singapore)

On-site comparison of Quantum Hall Effect resistance standards of the NMC A*STAR and the BIPM

⋅⬩⬥ Ongoing key comparison BIPM.EM-K12 ⬥⬩⋅

1. Introduction

The ongoing on-site key comparison BIPM.EM-K12 is part of the BIPM programme implemented to verify the international coherence of the primary resistance standards. It allows National Metrology Institutes (NMIs) to validate their implementations of the Quantum Hall Effect (QHE) for dc resistance traceability by comparison to the reference maintained at the BIPM.

In this comparison, the realization of the ohm from the QHE-based standard of the NMIs at 100 Ω is compared with that realized by the BIPM from its own transportable quantum Hall resistance standard. This comparison is normally completed by scaling measurements from 100 Ω to 1 Ω and 10 kΩ.

The comparison programme BIPM.EM-K12 started in 1993. A first series of five comparisons was carried out from this date until 1999. After a suspension period, the comparison was resumed in 2013. Since then five comparisons have been successfully completed whose results may be consulted on the webpage of the Key Comparison Data Base (KCDB) [1].

In March 2019 a new BIPM.EM-K12 comparison was carried out at the National Metrology Centre (NMC A*STAR), Singapore. It was the first time the NMC participated in this comparison program.

Only measurement results concerning the realization of the ohm at 100 Ω and the scaling to 10 kΩ will be presented in this report. The comparison results on the scaling to 1 Ω are not included in the report as the cryogenic comparison bridge used by the NMC A*STAR did not adequately match the current magnitude and cycle shape required by the scaling to 1 Ω comparison protocol. The application of a correction in order to compensate for the current waveform differences between the BIPM and the NMC measurements would have led to a measurement uncertainty at 1 Ω well beyond that expected in the BIPM.EM-K12 comparison.

2. Principle of the comparison measurements

The ohm can be reproduced from the QHE routinely with an accuracy of the order of 1 part in 10^9 or better. The present comparison is performed on-site in order to eliminate the limitation of transporting transfer resistance standards between the BIPM and the participating institute, which would otherwise result in an increase of the comparison uncertainty by at least a factor of 10.

To this end, the BIPM has developed a complete transportable system that can be operated at the participant's facilities to reproduce the ohm from a QHE reference at 100 Ω and scale this value to 1 Ω and 10 kΩ (meaning that not only the QHE systems are covered in this comparison but also the scaling devices).

For the reason given in the above introduction, only the calibration of the 100 Ω standard and scaling to 10 kΩ have been addressed in this comparison between the NMC and the BIPM. It then comprised only the two following stages, also schematized in Figure 1:

(i) The calibration of a 100 Ω standard resistor in terms of the QHE based standard of each of the institutes (NMC and BIPM). The conventional value $R_{\text{K-90}}$ is used to define the quantum Hall resistance value of both institutes. The relative difference in the calibrated values of the standard resistor of nominal value 100 Ω is expressed as $(R_{\text{NMC}} - R_{\text{BIPM}})/R_{\text{BIPM}}$ where R_{BIPM} and R_{NMC} are the values attributed by the BIPM and the NMC, respectively. The relative difference is independent of the value used for the von Klitzing constant and remains valid in the revised SI.

(ii) The scaling from 100 Ω to 10 kΩ through the measurement of the ratio $R_{10k\Omega}/R_{100\Omega}$ of the resistance of two standards of nominal value 10 kΩ and 100 Ω. The relative difference in the measurement of this ratio, hereinafter referred to as $K1$, is expressed as $(K1_{\mathrm{NMC}} - K1_{\mathrm{BIPM}})/K1_{\mathrm{BIPM}}$ where $K1_{\mathrm{BIPM}}$ and $K1_{\mathrm{NMC}}$ are the values attributed by the BIPM and the NMC, respectively.

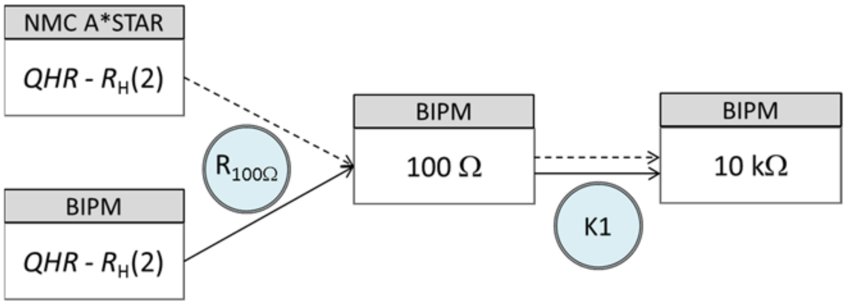

Figure 1: Schematic of the on-site comparison carried out at the NMC in March 2019. Rectangles represent the resistances to be compared and circles correspond to the resistance $R_{100\Omega}$ or the ratio $K1$ to be measured. Solid and dashed arrows stand for the measurements with the 1 Hz bridge of the BIPM or with the CCC bridge of the NMC, respectively.

The resistance value of each of the standard resistors used in this comparison is defined as the five- terminal dc-resistance value[1]. This means that it corresponds to the dc voltage-to-current ratio once any thermal emf across the resistor has reached a stable value.

3. The BIPM measurement system and the transfer standards

3.1. Implementation of the QHE

A complete transportable QHE reference [2] has been developed at the BIPM for the purpose of the BIPM.EM-K12 on-site comparison programme. It is composed of a compact liquid helium cryostat equipped with an 11 tesla magnet and a sample space that can be cooled to 1.3 K with the included vacuum pump. The superconducting magnet has an additional support at the bottom of the dewar to allow safe transport.

The separate sample probe can support two TO-8 mounted quantum Hall devices simultaneously (side by side within the magnet), with guarded wiring for eight terminals on each device. The BIPM uses GaAs heterostructure devices fabricated in the LEP 1990 EUROMET batch [3]. They give an i=2 plateau centered around 10.5 T which is well quantized for currents of at least 100 µA at 1.5 K. The cryostat and the QHE devices are suitable for a realization of the ohm meeting all the requirements of the CCEM guidelines [4] for a relative standard uncertainty down to 1×10^{-9}.

A transportable resistance bridge is used with the QHE cryostat for the measurement of the different resistance ratios being the subject of the comparison. It is based on a room-temperature low-frequency current comparator (LFCC) operated at 1 Hz (sinusoidal signal), meaning that all resistance or ratio measurements are carried out at 1 Hz by the BIPM during the comparison. That way to proceed is preferable to the transport of the BIPM Cryogenic Current Comparator (CCC) bridge on-site since the 1 Hz bridge is a more rugged instrument, simple to operate, and much less sensitive to electromagnetic interference and temperature variations. Furthermore, it provides resolution and reproducibility that are comparable to those achievable with the BIPM CCC bridge.

[1] Ratio of the voltage drop between the high and low potential terminals to the current flowing in the low current terminal, with the case - fifth terminal - maintained at the same potential as the low potential terminal

The 1 Hz bridge is equipped with two separate LFCCs of ratio 129:1 and 100:1, having turns 2065:16 and 1500:15. The construction and performances of these devices are detailed in [5,6].

3.2. Transfer standards

Two transfer resistance standards of value 100 Ω and 10 kΩ were used during the comparison. The values assigned by the BIPM and the NMC to the 100 Ω resistor in terms of R_{K-90} and to the ratio 10 kΩ/100 Ω are the measurands being compared in this comparison.

The transfer standards were provided by the BIPM. The 100 Ω standard was an IET Labs resistor of type SR102 (s/n: J2-1425644) and the 10 kΩ a Tegam resistor of type SR104 (s/n: K 201119630104). They are fitted in individual temperature-controlled enclosures held at 25°C. The temperature-regulation system can be powered either from the mains or from external batteries.

For each of these standards, the difference between resistance values measured at 1 Hz and at 'dc' is small but not negligible. These differences were determined at the BIPM prior to the comparison and checked afterwards. The 'dc' value was measured with the BIPM CCC whilst the 1 Hz value was measured with the transportable 1 Hz bridge (the same as that used on-site during the comparison). The differences are applied as corrections to the measurements performed at 1 Hz meaning that the 1 Hz bridge is used as a transfer instrument referenced to the BIPM CCC.

The frequency corrections (1 Hz-'dc') are reported in Table 1 for $R_{100\Omega}$ and $K1$. The main possible sources contributing to these corrections are the quantum Hall resistance (QHR), the 1 Hz bridge and the transfer standard itself. Nevertheless, at 1 Hz, the frequency dependence of the QHR is negligible compared to the comparison uncertainty [7], and the characterization of the bridge provides evidence that its error at 1 Hz is below 1 part in 10^9. Consequently, the frequency dependence observed is mainly attributed to the resistance standards themselves.

Resistance or resistance ratio	1 Hz–'dc' correction /10^{-9}	Standard uncertainty /10^{-9}
$(R_{100\Omega}(1\text{ Hz}) - R_{100\Omega}(\text{dc})) / 100$	-6.05	1.20
$(K1(1\text{ Hz}) - K1(\text{dc})) / 100$	-4.39	1.20

Table 1: Value of the 1 Hz to 'dc' corrections applied to the BIPM measurements carried out at 1 Hz (Value('dc')=Value(1 Hz)–Correction). These values are specific to the standards used in this comparison.

For the sake of completeness, it must be noticed that the 'dc' resistance value (or ratio) measured with the BIPM CCC bridge results from a current signal passing through the resistors having polarity reversals with a waiting time to zero between polarity inversions, cf. Figure 2. The polarity reversal frequency is of the order of 3 mHz (about 340 s cycle period) and the measurements are sampled only during 100 s before the change of polarity.

Previous characterization measurements of the $R_H(2)$/100 Ω and 10 kΩ/100 Ω ratios have shown that if the polarity reversal frequency is kept below 0.1 Hz, then, any effects of settling or ac behaviour remain of the order of 1 part in 10^9 or less.

However, in order to ensure the best possible comparability of the measurements performed by the BIPM and the participating institute, the measuring system of the latter should be configured to match as closely as possible the reference polarity reversal cycle of the BIPM CCC. In case this is not feasible, a correction should be estimated and applied to the participating NMI's measurements based either on additional characterization of the influence of the polarity reversal rate on the actual measured resistance ratio, or by any other means using the most relevant and reliable information available.

In that respect, in case different reversal current cycles (shape and/or magnitude) would be used by the BIPM and the NMI, an estimation of the difference of the effective powers dissipated in the resistance standards measured should be done and, if necessary, a correction applied taking into account the power coefficients of those standards.

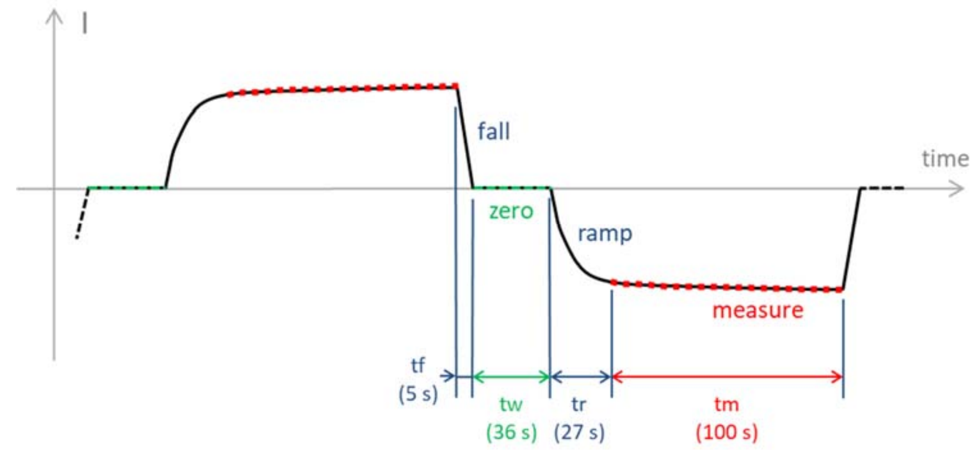

Figure 2: Schematic representation of the reference current cycle with polarity reversals used in the BIPM CCC bridge. Each half-cycle comprises a waiting time at zero current of 36 s, a ramp time of 27 s, a measuring (sampling) time of 100 s and a fall time of 5 s. The complete reversal cycle time is 336 s.

3.3. Uncertainty budget

Table 2 summarizes the BIPM standard uncertainties for the measurement of the 'dc' value of the 100 Ω standard in terms of the recommended value of the von Klitzing constant R_{K-90}, as well as the measurement uncertainties for the 10 kΩ/100 Ω ratio ($K1$).

Information about the imperfect realization of the ratio $R_H(2)$/100 Ω could be found in the references [5] and [7]. Further details about the ac measurement of the QHE will be found in the review paper [8].

Measurement Parameters	*Resistance ratio*	
	$R_H(2)$/100 Ω	10 kΩ/100 Ω
LFCC ratio	129/1	100/1
Current	40 µA/5.16 mA	50 µA/5 mA
Source of Uncertainty (type B)	*Relative standard uncertainties / 10^{-9}*	
Reference CCC bridge		
Imperfect CCC winding ratio	1.0	1.0
Resistive divider calibration	0.5	0.5
Leakage resistances	0.2	0.2
Noise rectification in CCC	1.0	1.0
Imperfect realization of the QHR	0.8	-
Correction of the 1 Hz-to 'dc' difference	1.2	1.2
Combined type B standard uncertainty, u_B=	**2.1**	**1.9**

Table 2: Contributions to the combined type B uncertainty for the 'dc' measurement of the two mentioned resistance ratios at the BIPM.

4. The NMC measurement system

4.1. Implementation of the QHE

The NMC primary reference of dc resistance is based on the Quantized Hall Resistance (QHR). The realized resistance value from the QHR is maintained by an ensemble of four 100 Ω reference resistance standards which are calibrated against the QHR using a cryogenic current comparator resistance bridge.

The QHR system consists of a low boil-off cryostat with a built in Helium-3 variable temperature insert (VTI) and a high-field superconducting magnet that produces fields up to 12 T. The VTI Helium-3 insert sample probe allows the experimental temperatures of the QHR sample to be maintained at temperature in the range from 0.3 K to 300 K.

The QHR samples typically operate on the i=2 plateau at a temperature between 0.3 K to 1.5 K and a magnetic flux density typically around 10.5 to 10.7 T. To ensure accurate measurements, the basic characterization checks detailed in [4] are performed on the sample before it is used in a measurement operation.

4.2. Resistance bridge

The CCC resistance bridge is based on a dual SQUID detectors design [9] for current and voltage balance null detection. The number of turns of the CCC matches the ratio for the QHR standard operating on the i=2 and i=4 plateaux against a 100 Ω resistor at 2065:16 for $R_H(2)$ to 100 Ω and 2065:32 for R_H (4) to 100 Ω, respectively. Common decade resistance ratios for comparing resistance from 1 Ω to 10 kΩ at 1:1, 1:10 and 1:100 ratios can be obtained by selecting various pairs of CCC windings to optimize the measurement result.

The CCC resistance bridge is capable to source current up to 20 mA. Nominal operating currents for $R_H(2)$ and $R_H(4)$ are at 23.245 µA and 46.489 µA respectively against the 100 Ω resistance standard at 3 mA. For resistance measurements, the current ratio is selected such that the maximum power dissipation in the resistors is maintained at 1 mW or less.

The shape of a typical current reversal cycle for the resistance measurement is schematized in Figure 3. The default configuration of a full cycle current reversal cycle is about 74 s. The reversal ramp time between the positive and negative current cycle is about 13 s with a zero current rest time *tw* of about 4 s. The measurement time *tm* is about 18 s with a settle time *ts* of 6 s.

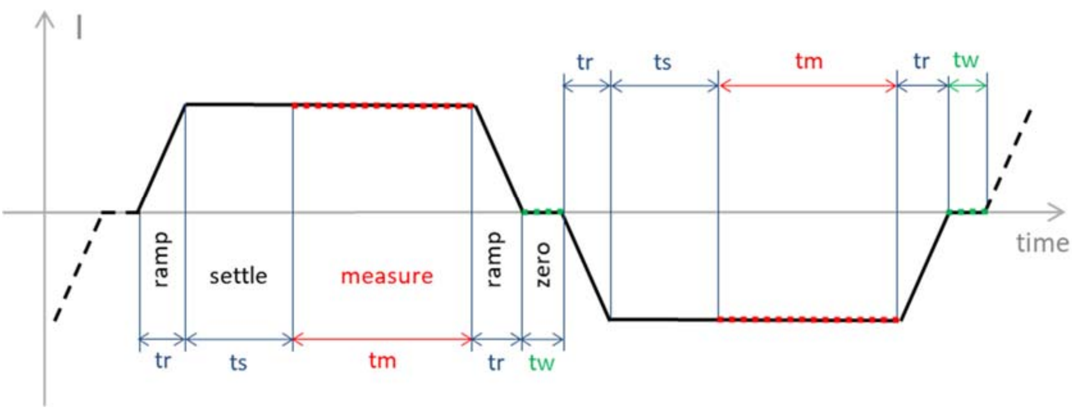

Figure 3: Standard current waveform and reversal cycle timing of the NMC CCC bridge. The ramp time (t_r), settle time (t_s), measurement time (t_m) and zero time (t_w) of the standard cycle used for measurements were 4.5 s, 6 s, 18 s and 4 s, respectively, for a total cycle period of 74 s.

4.3. Measuring environmental conditions

During the whole period of the comparison, the laboratory maintained an ambient temperature at (23±2) °C and relative humidity at (55±10) %. The atmospheric pressure during the comparison period from 13 to 18 March 2019 was in the range of 1005.9 hPa to 1007.5 hPa with a mean of 1007.0 hPa.

4.4. Uncertainty budget

The uncertainty budgets for the measurement of the 100 Ω resistance standard in terms of R_{K-90} and the 10 kΩ/100 Ω ratio ($K1$) are shown in Table 3.

Measurement Parameters	*Resistance ratio*	
	$R_H(2)$/100 Ω	10 kΩ/100 Ω
Number of turns N1/N2	2065/16	800/8
Current	23.25 µA/3 mA	0.03 mA/3 mA
Source of Uncertainty (type B)	*Relative standard uncertainties / 10^{-9}*	
CCC Resistance Bridge		
CCC ratio error	0.80	0.80
Leakage resistances	0.06	0.06
Calibration of balance	0.20	0.20
SQUID loop gain	0.35	0.35
Null Detector loop gain	0.35	0.35
Imperfect realization of R_H	2.00	-
Combined type B standard uncertainty, u_B=	**2.2**	**1.0**

Table 3: Contributions to the combined type B uncertainty for the NMC measurement of the two mentioned resistance ratios.

5. Measurement of the 100 Ω transfer standard in terms of $R_H(2)$

5.1. BIPM measurements

5.1.1. Preliminary tests

The quantum Hall sample used during the present comparison was operated on the i=2 plateau at a temperature of 1.3 K and with a rms current of 40 µA. The magnetic flux density corresponding to the middle of the plateau was determined by recording the longitudinal voltage V_{xx} versus flux density and was found to be 10.3 T. The two-terminal Hall resistance of the four-terminal-pairs device was checked before and after each series of measurements, showing that the contact resistance was smaller than a few ohms (and in any case not larger than 4 Ω - measurements limited by the resolution of the DVM used).
The absence of significant longitudinal dissipation along both sides of the device was tested as described in [4] section 6.2, by combining the measurements obtained from four different configurations of the voltage contacts (two opposite pairs in the center and at the end of the sample, and two diagonal configurations). The absence of dissipation was demonstrated within 5×10^{-10} in relative terms with a standard deviation of the same order. Subsequent series of measurements were taken from the central pair of contacts only.

5.1.2. BIPM results

As mentioned above, an rms current of 40 µA was drawn in the quantum Hall device. The current in the 100 Ω transfer standard was then 5.16 mA, corresponding to a Joule heating dissipation of about 2.66 mW.

After a preliminary set of measurements on March 12, 2019, five measurements of the 100 Ω standard were interleaved with five measurements by NMC on March 13, 2019. A difference of about 5×10^{-9} between NMC and BIPM was measured. This difference being higher than expected and NMC suspecting an issue with the operating temperature of their QHR, a second series of measurements was performed on March 14. However, a similar difference of about 4×10^{-9} was measured. On the same day, a test measurement of the $R_H(2)$/100 Ω ratio with the CCC bridge of the NMC but using the BIPM QHR gave a difference between NMC and BIPM of the order of 1×10^{-9}, showing that the issue was probably due to the QHE device used by NMC. A third series of interleaved measurements was then carried out on 18 March after the QHE sample of the NMC had been changed. More details about the chronological sequence of events are reported in section 5.2.

The measured 1 Hz and dc corrected values of the 100 Ω standard for the three series of measurements performed by the BIPM on March 13, 14 and 18 are reported in Table 4. They are expressed as the relative difference from the 100 Ω nominal value: (R_{BIPM}/100 Ω) - 1. Each measurement reported in the table is the mean value of a set of eight individual measurements corresponding to a total integration time of about 27 minutes.

Date	Time	(R_{BIPM}/100 Ω)-1 /10^{-6}		Dispersion /10^{-6}
		1 Hz measurements	'dc' corrected (1 Hz-'dc' correction)	
13/03/2019	13:22	2.382 4	2.3884	0.000 7
	15:06	2.380 9	2.3869	0.000 6
	16:42	2.382 0	2.3881	0.000 6
	18:18	2.381 2	2.3873	0.000 7
	20:18	2.380 0	2.3861	0.000 5
		Mean value =	**2.387 4**	
		Standard deviation, u_A =	**0.000 9**	
14/03/2019	11:47	2.385 8	2.391 9	0.000 5
	13:39	2.388 1	2.394 2	0.000 4
	15:32	2.387 7	2.393 7	0.000 6
	17:03	2.386 2	2.392 3	0.000 6
	19:22	2.386 2	2.392 3	0.000 7
		Mean value =	**2.392 9**	
		Standard deviation, u_A =	**0.001 0**	
18/03/2019	13:49	2.386 0	2.392 0	0.000 5
	15:37	2.385 8	2.391 9	0.000 5
	17:15	2.385 4	2.391 5	0.000 7
	19:41	2.386 2	2.392 2	0.000 5
		Mean value =	**2.391 9**	
		Standard deviation, u_A =	**0.000 3**	

Table 4: BIPM measurements of the 100 Ω standard in terms of $R_H(2)$, on March 13, 14 and 18, 2019. Each measurement corresponds to an integration time of about 27 minutes. Results are expressed as the relative difference from the nominal 100 Ω value. The time corresponds to the mean time of measurement and the dispersion to the standard deviation of the mean of the considered series of measurements.

The resistance values $\boldsymbol{R}_{\mathbf{BIPM}}$ reported below correspond to the means of the measurements carried out by the BIPM on each of the three days: March 13, 14 and 18, 2019.

March 13, 2019: Mean value: $\boldsymbol{R}_{\mathbf{BIPM}} = \mathbf{100 \times (1 + 2.387\,4 \times 10^{-6})\ \Omega}$

Relative standard uncertainty: $\boldsymbol{u}_{\mathbf{BIPM}} = \mathbf{2.3 \times 10^{-9}}$

where u_{BIPM} is calculated as the quadratic sum of $u_{\mathrm{A}} = 0.9 \times 10^{-9}$ and, from Table 2, $u_{\mathrm{B}} = 2.1 \times 10^{-9}$.

March 14, 2019: Mean value: $\boldsymbol{R}_{\mathbf{BIPM}} = \mathbf{100 \times (1 + 2.392\,9 \times 10^{-6})\ \Omega}$

Relative standard uncertainty: $\boldsymbol{u}_{\mathbf{BIPM}} = \mathbf{2.3 \times 10^{-9}}$

where u_{BIPM} is calculated as the quadratic sum of $u_{\mathrm{A}} = 1.0 \times 10^{-9}$ and, from Table 2, $u_{\mathrm{B}} = 2.1 \times 10^{-9}$.

March 18, 2019: Mean value: $\boldsymbol{R}_{\mathbf{BIPM}} = \mathbf{100 \times (1 + 2.391\,9 \times 10^{-6})\ \Omega}$

Relative standard uncertainty: $\boldsymbol{u}_{\mathbf{BIPM}} = \mathbf{2.1 \times 10^{-9}}$

where u_{BIPM} is calculated as the quadratic sum of $u_{\mathrm{A}} = 0.3 \times 10^{-9}$ and, from Table 2, $u_{\mathrm{B}} = 2.1 \times 10^{-9}$.

5.2. NMC measurements of $R_{\mathrm{H}}(2)/100\ \Omega$

5.2.1. Sequence of measurements

The GaAs-based QHR sample referenced “3P” was initially used by NMC for this comparison. The sample was operated on the i=2 plateau at a current of 23.245 μA. The magnetic flux density corresponding to the centre of the plateau was 10.7 T with the absence of significant longitudinal dissipation along both sides of the device tested. Contact resistances were measured to be less than 1 Ω.

The 100 Ω resistance standard was measured with a current of 3 mA. The current reversal cycle for the resistance measurement was set at a full standard cycle of 74 s (Figure 3). As both the current magnitude and wave shape are different from those used by the BIPM, the NMC measurement results were corrected for the difference of the effective powers dissipated in the 100 Ω standard (‘power’ corrected measurements in Tables 5 and 6). The estimation of this correction is detailed in section 5.2.2.

The Helium-3 insert sample probe encountered an operational issue during the starting of the comparison on March 13, 2019 and resulted in the operating temperature of the QHR sample reaching about 1.6 K in the beginning of the measurements and around 1.9 K at the end of the day.

Five measurements by NMC, interleaved with five BIPM measurements were conducted on March 13, 2019. The first measurement was carried out with the 100 Ω standard temperature control system powered by mains. All remaining NMC measurements during the comparison were performed with the 100 Ω standard’s temperature control system powered on battery. Each NMC measurement consisted of a set of five independent measurements. Each of these independent measurements consisted of five current reversal measurement cycles corresponding to a total time of about 6 minutes. Each NMC measurement lasted then about 31 minutes (for a sampling time 15 minutes).

The raw and ‘power’ corrected measurement results obtained on March 13 are shown in Table 5 along with the mean time of measurement and dispersion (standard deviation of the mean). A preliminary check on the difference with BIPM’s measurements of the 100 Ω standard indicated a mean relative difference larger than what could be expected, in the order of 5×10^{-9}.

The Helium-3 insert sample probe was brought up to room temperature overnight and cooled down again on March 14, 2019. However, the issue with the operating temperature remained and the QHR sample was at 1.6 K at the beginning of the measurements and around 1.8 K at the end of the day. It was also discovered that the cable connecting the 100 Ω standard to the CCC resistance bridge had a poor joint at the connecting copper spade terminal and the cable was replaced.

The magnetic flux density corresponding to the centre of the plateau was the same as the day before (10.7 T). The absence of significant longitudinal dissipation along both sides of the device was tested and the contact resistances measured to be less than 1 Ω. Four measurements by NMC, interleaved with BIPM measurements, were conducted in the same experimental conditions as on March 13, except that each NMC measurement consisted of a set of six independent measurements. The measurement results are reported in Table 5. The comparison of the mean of the NMC and BIPM interleaved measurements shown a difference slightly lower of about 4×10^{-9}, but still higher than it could be expected.

Date	Time	$(R_{\mathrm{NMC}}/100\ \Omega)-1$ /10^{-6}		Dispersion /10^{-6}
		Raw measurements	‘Power’ corrected	
13/03/2019	11:51	2.383 1	2.382 8	0.001 4
	14:11	2.382 2	2.381 9	0.003 7
	16:03	2.382 3	2.382 0	0.001 5
	17:33	2.383 1	2.382 8	0.001 5
	19:06	2.381 1	2.380 8	0.004 1
		Mean value =	**2.382 1**	
		Standard deviation, u_A =	**0.000 8**	
14/03/2019	12:42	2.392 0	2.391 7	0.000 1
	14:47	2.388 2	2.387 9	0.001 4
	16:20	2.388 2	2.387 9	0.000 4
	18:11	2.388 2	2.387 9	0.000 2
		Mean value =	**2.388 9**	
		Standard deviation, u_A =	**0.001 9**	

Table 5: NMC measurements of the 100 Ω standard in terms of $R_{\mathrm{H}}(2)$ using **QHR device referenced ‘3P’**, on March 13 and 14, 2019. Each measurement corresponds to an integration time of 15 minutes. Results are expressed as the relative difference from the nominal 100 Ω value. The time corresponds to the mean time of measurement and the dispersion to the standard deviation of the mean of the considered series of five independent measurements.

In order to determine if the measured BIPM-NMC difference was due to the unusual operating temperature of the NMC’s QHR, a quick measurement of the 100 Ω resistance standard was carried out using NMC’s CCC resistance bridge and the BIPM QHR resistance as reference standard. The result shown a reduction of the difference to the range of 1×10^{-9}. This finding suggested that there may be imperfect quantization of NMC’s QHR sample and possible degrading of this sample due to temperature dependence that may be affected by operating it at a temperature higher than the usual 0.3 K to 1.5 K range.

A repeat measurement of the 100 Ω standard was carried out on March 18, 2019 with another QHR sample referenced “1P”. The wiring and assembly of the Helium-3 insert sample probe were carefully inspected before being mounted into the VTI with the QHR sample. An operating temperature of the QHR sample of about 0.3 K could be reached after cooling of the Helium-3 insert sample probe.

The sample was operated on the i=2 plateau at a current of 23.245 µA. The magnetic flux density corresponding to the centre of the plateau was 10.5 T with the absence of significant longitudinal dissipation along both sides of the device tested. Contact resistances were measured to be less than 1 Ω.

Four NMC measurements using the QHR sample "1P" interleaved with five BIPM measurements were planned. At the end of the third NMC measurements, the laboratory experienced an unexpected power failure due to tripping of the circuit breaker at the central switchboard that was triggered by a facility located next to the laboratory. The power to the laboratory was restored about an hour later but the disruption of the cryogenic system operation had caused the pressure to build up in the cryostat and temperature of the NMC QHR sample had raised significantly. The temperature of the sample could only be reduced to around 2.1 K about an hour after the system cryostat resumed its operation. Resistance measurements showed a relative decrease of about 3×10^{-7} in the 100 Ω resistance values with a large unstable dispersion.

Regarding the BIPM system, after having resumed pumping on the sample chamber of their cryostat, the normal operating temperature of the QHR was restored and no effect of the power shutdown was detected on the measurement of the $R_H(2)/100$ Ω ratio. A fourth measurement could be carried out by the BIPM.

The issue with the NMC's cryostat forced a stop to the current comparison series of interleaved measurements. As both the NMC and the BIPM measurements didn't show unusual dispersion or drift, it was decided that the four BIPM measurements, interleaved with the three first NMC measurements, were enough for the comparison (moreover, the limited time duration of the comparison wouldn't have allowed to repeat once again a series of $R_H(2)/100$ Ω measurements). The mean of the four BIPM measurements was then compared to the mean of the three NMC measurements showing the difference between NMC and BIPM had reduced to less than 2×10^{-9}. The use of the QHE device '1P' had improved significantly the 100 Ω measurements from NMC. Only this series has been kept for the comparison.

The temperature of the NMC QHR sample was about 300 mK in the beginning and 1.5 K at the end of the third measurement. The raw and 'power' corrected measurement results are reported in Table 6.

Date	Time	(R_{NMC}/100 Ω)-1 /10^{-6}		Dispersion /10^{-6}
		Raw measurements	'Power' corrected	
18/03/2019	14:48	2.393 6	2.393 3	0.001 4
	16:30	2.394 1	2.393 8	0.002 1
	18:10	2.393 7	2.393 4	0.001 2
	20:33	2.116 8	2.116 5	0.018 4
		Mean value =	**2.393 5**	
		Standard deviation, u_A =	**0.000 3**	

Table 6: NMC measurements of the 100 Ω standard in terms of $R_H(2)$ using **QHR device referenced '1P'** on March 18, 2019. Each measurement corresponds to an integration time of 15 minutes. Results are expressed as the relative difference from the nominal 100 Ω value. The time corresponds to the mean time of measurement and the dispersion to the standard deviation of the mean of the considered series of measurements. The last measurement (20:33), performed after the power shutdown, has not been taken into account for the computation of the mean value and of the standard deviation u_A.

.../...

The resistance values $\boldsymbol{R}_{\mathbf{NMC}}$ reported below correspond to the mean of the ratio measurements carried out by the NMC corrected from power difference dissipated in the 100 Ω (see section 5.2.2), on each of the three days: March 13, 14 and 18, 2019.

March 13, 2019: Mean value: $\boldsymbol{R}_{\mathbf{NMC}} = \mathbf{100 \times (1 + 2.382\ 1 \times 10^{-6})\ \Omega}$

Relative standard uncertainty: $\boldsymbol{u}_{\mathbf{NMC}} = \mathbf{2.7 \times 10^{-9}}$

where u_{NMC} is calculated as the quadratic sum of: $u_{\mathrm{A}} = 0.8 \times 10^{-9}$, $u_{power} = 1.3 \times 10^{-9}$ the standard uncertainty on power correction and, from Table 3, $u_{\mathrm{B}} = 2.2 \times 10^{-9}$.

March 14, 2019: Mean value: $\boldsymbol{R}_{\mathbf{NMC}} = \mathbf{100 \times (1 + 2.388\ 9 \times 10^{-6})\ \Omega}$

Relative standard uncertainty: $\boldsymbol{u}_{\mathbf{NMC}} = \mathbf{3.2 \times 10^{-9}}$

where u_{NMC} is calculated as the quadratic sum of: $u_{\mathrm{A}} = 1.9 \times 10^{-9}$, $u_{power} = 1.3 \times 10^{-9}$ the standard uncertainty on power correction and, from Table 3, $u_{\mathrm{B}} = 2.2 \times 10^{-9}$.

March 18, 2019: Mean value: $\boldsymbol{R}_{\mathbf{NMC}} = \mathbf{100 \times (1 + 2.393\ 5 \times 10^{-6})\ \Omega}$

Relative standard uncertainty: $\boldsymbol{u}_{\mathbf{NMC}} = \mathbf{2.6 \times 10^{-9}}$

where u_{NMC} is calculated as the quadratic sum of: $u_{\mathrm{A}} = 0.3 \times 10^{-9}$, $u_{power} = 1.3 \times 10^{-9}$ the standard uncertainty on power correction and, from Table 3, $u_{\mathrm{B}} = 2.2 \times 10^{-9}$.

5.2.2. Estimation of the power correction of NMC measurements

Given that BIPM and NMC measurements were made at different current magnitudes and for different reversal cycle shapes and timing (cf. Figures 2 and 3), the non-zero power coefficient of the 100 Ω standard can affect the computed difference between NMC and BIPM measurements.

In order to take into account the difference of effective powers dissipated in the 100 Ω, an estimation of its power coefficient was performed by the BIPM during the comparison. This estimation was deduced from the measurement of the $R_{\mathrm{H}}(2)/100\ \Omega$ ratio at different applied currents and was found to be equal to -0.24 parts in 10^9 per mW, with a standard uncertainty of 1.27 parts in 10^9.

From the current magnitudes and reversal cycle shapes used by the BIPM and NMC CCC bridges, it was estimated that the effective power dissipated in 100 Ω by the BIPM was 1.20 mW higher than that dissipated by NMC. Considering the power coefficient of the 100 Ω given above, a power correction was computed and applied to the NMC measurement results (Tables 5 and 6). This correction was estimated to be (-0.29 ± 1.27) parts in 10^9.

5.3. 100 Ω measurements comparison

For the sake of completeness, Figures 4, 5 and 6 present the corrected interleaved measurements from NMC and BIPM on March 13, 14 and 18, 2019, respectively (from data in Tables 4, 5 and 6). However, as explained in section 5.2.1, considering that the NMC's QHR device referenced '3P' was defective or operated in inappropriate experimental conditions, only the measurement results from March 18, 2019 were considered for the comparison.

On that day, before the power shutdown, no significant instabilities of the 100 Ω transfer resistor were observed within the limit of the dispersion of the results (Figure 6). Therefore, no additional uncertainty component was included in the final comparison results.

The difference between NMC and BIPM was then calculated as the difference of the means of the series of measurements carried out by both institutes (mean values reported in Tables 4 and 6):

Relative difference NMC-BIPM: $\mathbf{(}\boldsymbol{R}_{\mathbf{NMC}}\mathbf{-}\boldsymbol{R}_{\mathbf{BIPM}}\mathbf{)\ /\ }\boldsymbol{R}_{\mathbf{BIPM}}\mathbf{= 1.6 \times 10^{-9}}$

Relative combined standard uncertainty: $\boldsymbol{u}_{\mathbf{comp}}\mathbf{= 3.3 \times 10^{-9}}$

where u_{comp} is calculated as the quadratic sum of $u_{\mathrm{BIPM}} = 2.1 \times 10^{-9}$ and $u_{\mathrm{NMC}} = 2.6 \times 10^{-9}$.

Notice that the above value of u_{NMC} includes the power correction uncertainty resulting from the different effective powers dissipated in the 100 Ω standard during the comparison measurements. In standard NMC conditions, u_{NMC} would have been reduced to 2.2×10^{-9}.

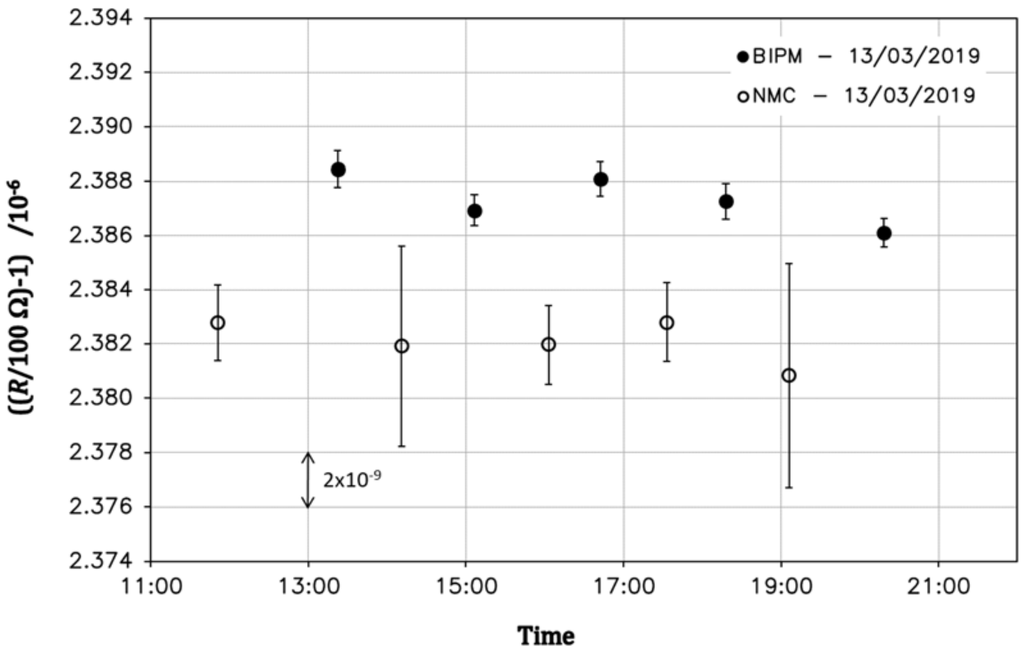

Figure 4: NMC (open circles) and BIPM (black dots) corrected measurements of the 100 Ω resistance R in terms of $R_{\mathrm{H}}(2)$ on March 13, 2019. NMC measurements were performed with the **QHR device referenced '3P'**, the temperature of which varied from 1.6 K to 1.9 K between beginning and end of the measurement series. The error bars correspond to the dispersion observed during each measurement.

…/…

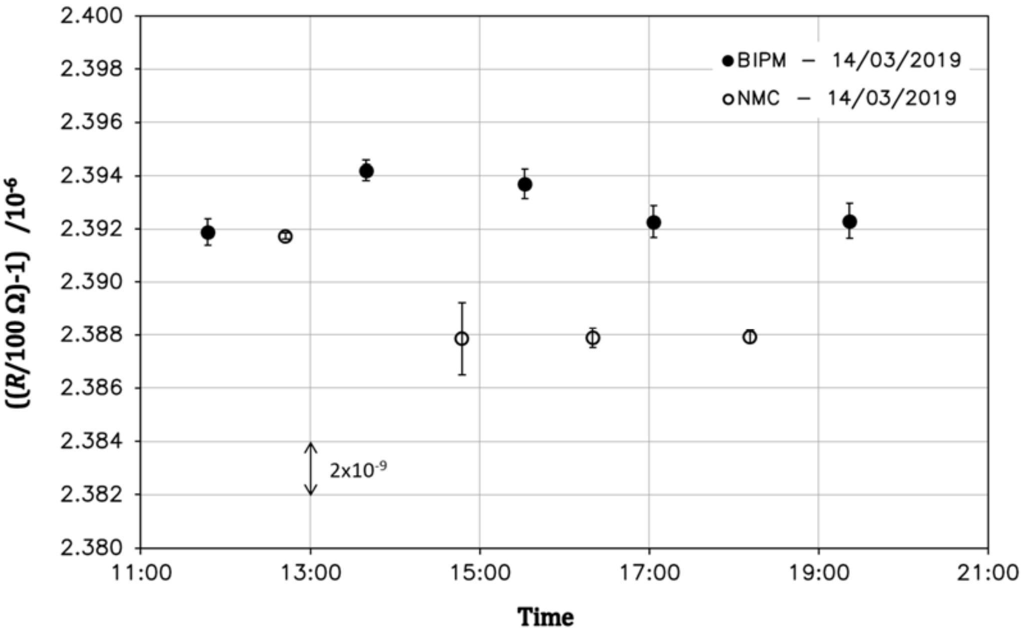

Figure 5: NMC (open circles) and BIPM (black dots) corrected measurements of the 100 Ω resistance R in terms of $R_{\mathrm{H}}(2)$ on March 14, 2019. NMC measurements were performed with the **QHR device referenced '3P'**, the temperature of which varied from 1.6 K to 1.8 K between beginning and end of the measurement series. The error bars correspond to the dispersion observed during each measurement.

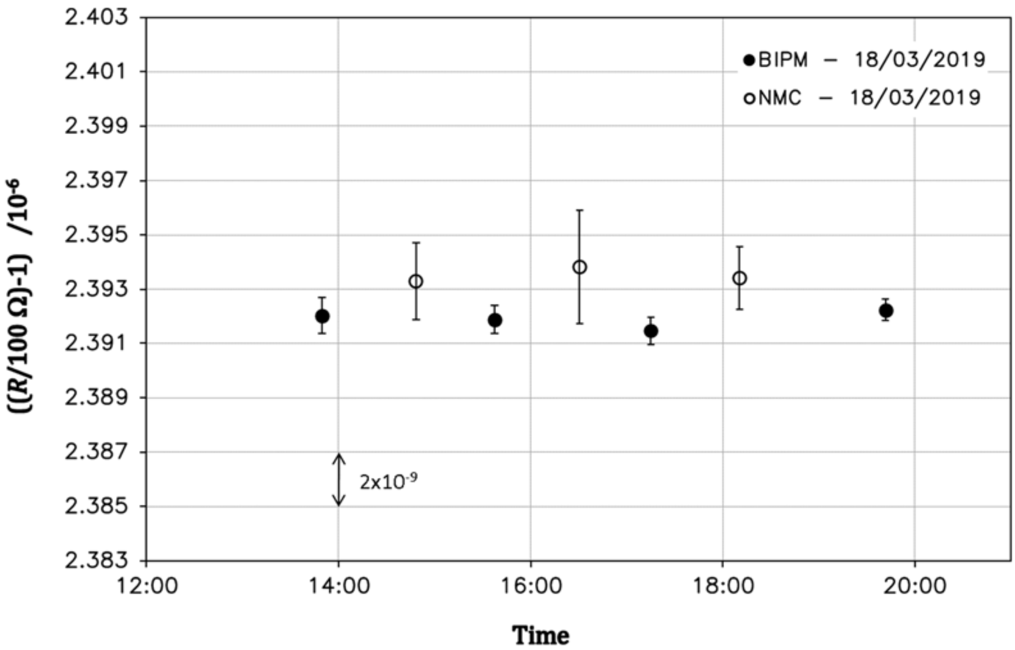

Figure 6: NMC (open circles) and BIPM (black dots) corrected measurements of the 100 Ω resistance R in terms of $R_{\mathrm{H}}(2)$ on March 18, 2019. NMC measurements were performed with the **QHR device referenced '1P'**, the temperature of which varied from 0.3 K to 1.5 K between beginning and end of the measurement series. The error bars correspond to the dispersion observed for each measurement.

6. Measurement of the ratio *K*1 (10 kΩ/100 Ω)

6.1. BIPM measurements of *K*1

For the measurement of the *K*1 ratio the 129:1 LFCC equipping the BIPM 1 Hz bridge for $R_H(2)$/100 Ω ratio measurement was replaced by a 100:1 LFCC. The rms current in the 10 kΩ standard was 50 μA corresponding to 5 mA in the 100 Ω standard. The temperature control electronics of the two resistance standards were powered using batteries. The standards were connected alternately to the BIPM and NMC bridges and five BIPM measurements at 1 Hz were interleaved with four NMC measurements.

The measurements were carried out on March 15, 2019. Each of the five BIPM measurements, reported in Table 7, corresponds to the mean value of eight individual measurements corresponding to a total integration time of about 27 minutes. The 1 Hz - dc correction applied on raw measurements is given in Table 1, section 3.2. The dispersion corresponds to the standard deviation of the mean of the eight individual measurements.

Date	Time	$(K1_{BIPM}/100)-1$ /10^{-6}		Dispersion /10^{-6}
		1 Hz measurements	'dc' corrected (1 Hz-'dc' correction)	
15/03/2019	14:29	-1.105 3	-1.100 9	0.000 7
	16:28	-1.105 5	-1.101 1	0.000 5
	18:03	-1.107 2	-1.102 8	0.000 4
	19:40	-1.106 9	-1.102 5	0.000 6
	21:13	-1.106 8	-1.102 4	0.000 6
		Mean value =	**-1.102 0**	
		Standard deviation, u_A =	**0.000 9**	

Table 7: BIPM measurements of the ratio *K*1 (10 kΩ/100 Ω) on March 15, 2019. Each measurement corresponds to an integration time of about 27 minutes. Results are expressed as the relative difference from the nominal ratio value 100. The time corresponds to the mean time of measurement and the dispersion to the standard deviation of the mean of the considered series of measurements.

The *K*1 ratio value reported below correspond to the mean of the ratio measurements carried out by the BIPM on March 15, 2019.

Mean value: $\boldsymbol{K1_{BIPM} = 100 \times (1 - 1.102\,0 \times 10^{-6})}$

Relative standard uncertainty: $\boldsymbol{u_{BIPM} = 2.1 \times 10^{-9}}$

where u_{BIPM} is calculated as the quadratic sum of $u_A = 0.9 \times 10^{-9}$ and, from Table 2, $u_B = 1.9 \times 10^{-9}$.

6.2. NMC measurements of *K*1

For the measurement of *K*1, the standard 74 s current reversal cycle of Figure 3 was also used. The measurement currents through the 100 Ω and 10 kΩ resistance standards were 3 mA and 0.03 mA, respectively. The turns ratio of the NMC CCC resistance bridge was set to 800/8.

Both the current magnitude and waveform used by the NMC and the BIPM for the measurement of *K*1 were different. The difference of effective powers dissipated in the resistance standards has then been considered and a 'power' correction estimated and applied to NMC measurements.

As no influence on the measurement of $K1$ was expected from the difference of the currents driven in the 10 kΩ standard (50 µA and 30 µA for BIPM and NMC, respectively), only the difference of effective powers dissipated in the 100 Ω standard has been taken into account. This difference was estimated to 1.09 mW and, considering the power coefficient of the 100 Ω estimated in 5.2.2, a correction of (0.26 ± 1.27) × 10^{-9} was estimated for the ratio $K1$ measured by NMC.

As mentioned earlier, four NMC measurements interleaved with five BIPM measurements were conducted on March 15, 2019. Each of the NMC measurement consisted of a set of 6 independent measurements, consisting themselves of 5 current reversal measurement cycles corresponding to a measurement time of about 6 minutes. The total integration time of one NMC measurement was then 18 minutes (36 s integration time per cycle, times 5 cycles, times 6 measurements) for a total measurement time of about 37 minutes.

The raw and 'power' corrected measurement results of NMC are reported in Table 8. They are expressed as the relative difference from the nominal ratio value 100 with a dispersion corresponding to the standard deviation of the mean of the 6 individual measurements.

Date	Time	$(K1_{NMC}/100)-1$ /10^{-6}		Dispersion /10^{-6}
		Raw measurements	'Power' corrected	
15/03/2019	15:36	-1.104 0	-1.103 7	0.001 7
	17:17	-1.104 1	-1.103 8	0.001 3
	18:57	-1.105 6	-1.105 3	0.003 0
	20:28	-1.103 2	-1.102 9	0.003 1
		Mean value =	**-1.104 0**	
		Standard deviation, u_A =	**0.001 0**	

Table 8: NMC measurements of the ratio $K1$ (10 kΩ/100 Ω) on March 15, 2019. Each measurement corresponds to an integration time of 18 minutes. Results are expressed as the relative difference from the nominal ratio value 100. The time corresponds to the mean time of measurement and the dispersion to the standard deviation of the mean of the considered set of measurements.

The $K1$ ratio value reported below correspond to the mean of the ratio measurements carried out by the NMC on March 15, 2019.

Mean value: $\boldsymbol{K1_{NMC} = 100 \times (1 - 1.104\,0 \times 10^{-6})}$

Relative standard uncertainty: $\boldsymbol{u_{NMC} = 1.9 \times 10^{-9}}$

where u_{NMC} is calculated as the quadratic sum of u_A =1.0 × 10^{-9} , u_{power} = 1.3 × 10^{-9} the standard uncertainty on power correction and, from Table 3, u_B = 1.0 × 10^{-9}.

6.3. Comparison of $K1$ measurements

Figure 7 presents the corrected measurements from NMC and BIPM on March 15, 2019 (data from Tables 7 and 8). Error bars correspond to the dispersion observed for each measurement.

No significant instabilities of the measured ratio $K1$ were observed within the limit of the dispersion of the results (Figure 7). Therefore, no additional uncertainty component was included in the final comparison results.

The difference between NMC and BIPM can then be calculated as the difference of the means of the series of measurements carried out by both institutes (mean values reported in Tables 7 and 8):

Relative difference NMC-BIPM: $\mathbf{(\mathit{K}1_{NMC} - \mathit{K}1_{BIPM}) / \mathit{K}1_{BIPM} = -2.0 \times 10^{-9}}$

Relative combined standard uncertainty: $\mathbf{u_{comp} = 2.8 \times 10^{-9}}$

where u_{comp} is calculated as the quadratic sum of $u_{\mathrm{BIPM}} = 2.1 \times 10^{-9}$ and $u_{\mathrm{NMC}} = 1.9 \times 10^{-9}$.

Notice that the above value of u_{NMC} includes the power correction uncertainty resulting from the different effective powers dissipated in the 100 Ω standard during the comparison measurements. In standard NMC conditions, u_{NMC} would have been reduced to 1.4×10^{-9}.

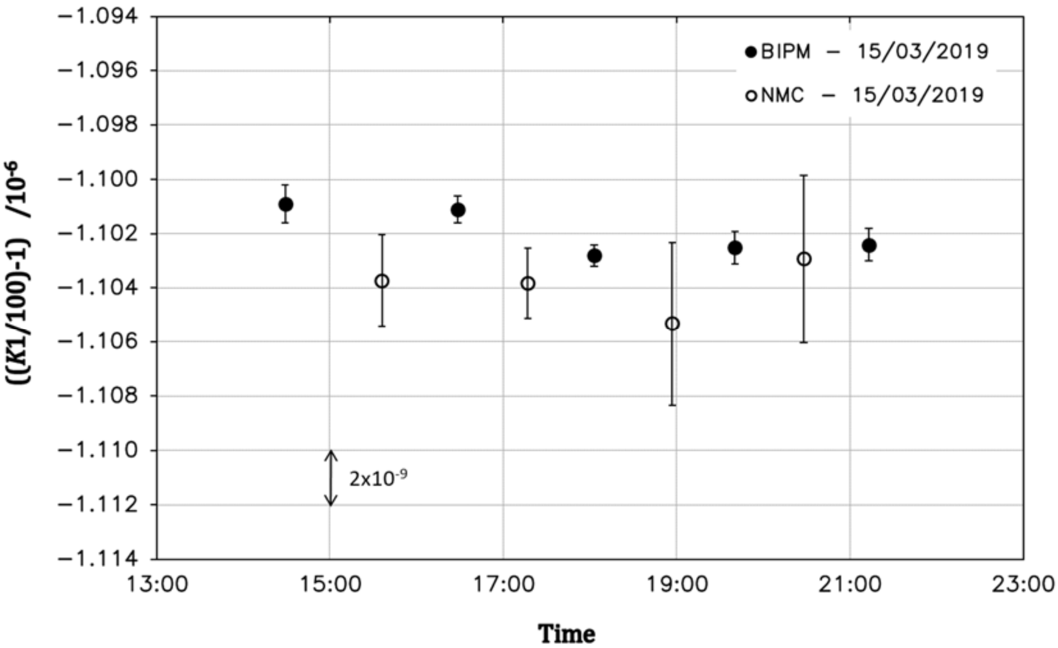

Figure 7: NMC (open circles) and BIPM (black dots) corrected measurements of the ratio $K1$ (10 kΩ/100 Ω) on March 15, 2019. The error bars correspond to the dispersion observed during each measurement.

7. Conclusion

The on-site key comparison BIPM.EM-K12 carried out from March 13 to March 18, 2019 between the BIPM and the NMC showed good agreement in the measurements of a conventional 100 Ω resistor in terms of the quantized Hall resistance ($R_{\mathrm{H}}(2)$), and in the determination of the resistance ratio 10 kΩ/100 Ω ($K1$).

The comparison results for the measurement of $R_{100\Omega}$ in terms of $R_{\mathrm{H}}(2)$ and of $K1$ ratio are summarized in Table 12.

$R_{100\Omega}$ in terms of $R_{\mathrm{H}}(2)$	$(R_{\mathrm{NMC}} - R_{\mathrm{BIPM}}) / R_{\mathrm{BIPM}} = \mathbf{1.6 \times 10^{-9}}$	$u_{\mathrm{comp}} = \mathbf{3.3 \times 10^{-9}}$
$K1 = R_{10\mathrm{k}\Omega}/R_{100\Omega}$	$(K1_{\mathrm{NMC}} - K1_{\mathrm{BIPM}}) / K1_{\mathrm{BIPM}} = \mathbf{-2.0 \times 10^{-9}}$	$u_{\mathrm{comp}} = \mathbf{2.8 \times 10^{-9}}$

Table 12: Summary of the results and associated relative standard uncertainties of the NMC-BIPM onsite comparison BIPM.EM-K12.

The above results will also appear as Degree of Equivalence (DoE) in the BIPM Key Comparison Database (KCDB). The DoE of the participating institute with respect to the reference value is given by a pair of terms: the difference D from the reference value and its expanded uncertainty for k=2, i.e. U=2u. The reference value of the on-going comparison BIPM.EM-K12 was chosen to be the BIPM value.

The comparison results expressed as DoEs are summarized in Table 13.

	Degree of equivalence D /10^{-9}	Expanded uncertainty U /10^{-9}
$R_{100\Omega}$ in terms of $R_{\mathrm{H}}(2)$	**1.6**	**6.6**
$K1 = R_{10\mathrm{k}\Omega}/R_{100\Omega}$	**-2.0**	**5.6**

Table 13: Summary of the comparison results expressed as degrees of equivalence (DoEs): difference from the BIPM reference value and expanded uncertainty U (k=2).

References

[1] http://kcdb.bipm.org/appendixb/KCDB_ApB_search.asp.

[2] F. Delahaye, T.J. Witt, F. Piquemal and G. Genevès, "Comparison of quantum Hall effect resistance standards of the BNM/LCIE and the BIPM", *IEEE Trans on Instr. and Meas.*, Vol. 44, n°2, 1995, 258-261.

[3] F. Piquemal, G. Genevès, F. Delahaye, J.P. André, J.N. Patillon and P. Frijlink, "Report on a joint BIPM-EUROMET project for the fabrication of QHE samples by the LEP", *IEEE Trans on Instr. and Meas.*, Vol. 42, n°2, 1993, 264-268.

[4] F. Delahaye and B. Jeckelmann, "Revised technical guidelines for reliable dc measurements of the quantized Hall resistance", *Metrologia*, 40, 2003, 217-223.

[5] F. Delahaye and D. Bournaud, "Accurate ac measurements of standard resistors between 1 and 20 Hz", *IEEE Trans on Instr. and Meas.*, Vol. 42, n°2, 1993, 287-291.

[6] A. Satrapinski, M. Götz, E. Pesel, N. Fletcher, P. Gournay, B. Rolland, "New Generation of Low-Frequency Current Comparators Operated at Room Temperature", *IEEE Trans. on Instr. and Meas.*, Vol. 66, n°6, 2017, 1417-1424.

[7] F. Delahaye, "An ac-bridge for low frequency measurements of the quantized Hall resistance", *IEEE Trans. on Instr. and Meas.*, Vol. 40, n°6, 1991, 883-888.

[8] F. Ahlers, B. Jeanneret, F. Overney, J. Schurr and B. Wood, "Compendium for precise ac measurements of the quantum Hall resistance", *Metrologia*, 46/5, 2009, R1-R11.

[9] J M Williams, P D Patel, T Holubar, and J Good, "Cryogenic Current Comparator Bridge with Dual SQUID Detectors", *Proceeding of the 29th Conference on Precision Electromagnetic Measurements (CPEM 2014)*, 24-29 Aug. 2014, 694-695.